ARMY RESEARCH LABORATORY

Characterization Techniques Employed to Determine the Energy Release of Reactive Materials

by John J. Ritter, Andrew L. Brant, Joseph W. Colburn, Barrie E. Homan, and Kevin L. McNesby

ARL-TR-5125 **March 2010**

NOTICES

Disclaimers

The findings in this report are not to be construed as an official Department of the Army position unless so designated by other authorized documents.

Citation of manufacturer's or trade names does not constitute an official endorsement or approval of the use thereof.

Destroy this report when it is no longer needed. Do not return it to the originator.

Army Research Laboratory
Aberdeen Proving Ground, MD 21005-5066

ARL-TR-5125 **March 2010**

Characterization Techniques Employed to Determine the Energy Release of Reactive Materials

John J. Ritter, Andrew L. Brant, Joseph W. Colburn,
Barrie E. Homan, and Kevin L. McNesby
Weapons and Materials Research Directorate, ARL

REPORT DOCUMENTATION PAGE

Form Approved
OMB No. 0704-0188

1. REPORT DATE *(DD-MM-YYYY)*	2. REPORT TYPE	3. DATES COVERED (From - To)
March 2010	Final	July 2008 to July 2009

4. TITLE AND SUBTITLE
Characterization Techniques Employed to Determine the Energy Release of Reactive Materials

5a. CONTRACT NUMBER

5b. GRANT NUMBER

5c. PROGRAM ELEMENT NUMBER

6. AUTHOR(S)
John J. Ritter, Andrew L. Brant, Joseph W. Colburn, Barrie E. Homan, and Kevin L. McNesby

5d. PROJECT NUMBER

5e. TASK NUMBER

5f. WORK UNIT NUMBER

7. PERFORMING ORGANIZATION NAME(S) AND ADDRESS(ES)
U.S. Army Research Laboratory
ATTN: RDRL-WML-D
Aberdeen Proving Ground, MD 21005-5066

8. PERFORMING ORGANIZATION REPORT NUMBER
ARL-TR-5125

9. SPONSORING/MONITORING AGENCY NAME(S) AND ADDRESS(ES)

10. SPONSOR/MONITOR'S ACRONYM(S)

11. SPONSOR/MONITOR'S REPORT NUMBER(S)

12. DISTRIBUTION/AVAILABILITY STATEMENT
Approved for public release; distribution unlimited.

13. SUPPLEMENTARY NOTES

14. ABSTRACT
Reactive materials show a promising future in an assortment of Army weapons systems due to their unique material characteristics. They have the potential to provide for enhanced lethality over their conventional munitions counterparts. However, those characteristics are not well defined, particularly the materials' fundamental energy release mechanisms. Through live fire experimental testing of an array of reactive materials consisting of an Al-Ni base, energy release characteristics can be understood on a more scientific level. This is accomplished through the incorporation of customized diagnostic techniques. Test samples of reactive material are fired via a powder gun into a steel-enclosed test chamber fitted with a polycarbonate window for witnessing the event. Raw data from the reaction event is recorded via high speed cameras and oscilloscopes. Analytical tools that are incorporated to characterize the event include pressure measurement gages, high speed imaging, pyrometry, spectroscopy, and flash x-ray. Through a systematic, scientific approach the vast amounts of data collected using these diagnostic tools is then processed into practical information of the reactive material's energy release behavior.

15. SUBJECT TERMS
Reactive material; energy release; optical diagnostics

16. SECURITY CLASSIFICATION OF:			17. LIMITATION OF ABSTRACT	18. NUMBER OF PAGES	19a. NAME OF RESPONSIBLE PERSON
a. REPORT	b. ABSTRACT	c. THIS PAGE			John J. Ritter
Unclassified	Unclassified	Unclassified	UU	34	19b. TELEPHONE NUMBER (*Include area code*) (410) 306-0709

Standard Form 298 (Rev. 8/98)
Prescribed by ANSI Std. Z39.18

Contents

List of Figures

Acknowledgments

The authors would like to thank General Sciences, Inc. for the material samples used in testing. Also, special thanks to Zachary Quine for his overall assistance during testing.

INTENTIONALLY LEFT BLANK.

1. Introduction

The U.S. Army has a critical need for increased lethality while maintaining an objective for green and insensitive munitions. Reactive materials (RMs) have been identified as a possible solution to this need as they can efficiently couple their energy into existing and novel lethality mechanisms. RMs, with the potential of high densities and materials strengths, have the potential to replace the parasitic materials that are integral to almost all current munitions designs providing enhanced performance and lower sensitivities. Reactive materials having theoretical energy densities, much higher than conventional explosives, can achieve insensitivity because they are not detonable, or are highly insensitive. Understanding the energy release mechanisms of these materials is key to fully exploiting their unique characteristics. Using an array of diagnostic tools and techniques, information can be gathered about the energy release mechanisms in reactive materials. Data, primarily collected through optical devices, is analyzed to provide scientific insight into the reactive material's energy release process. Similar reactive material characterization efforts have been put forth by the Navy and Air Force (*1*, *2*), however, the Army's efforts are unique in that they rely primarily on measuring the reaction event using optical techniques. For this discussion, the materials tested consisted of an Al-Ni matrix with complete, detailed data results available (*3*).

2. Test Setup

The reactive material energy release characterization testing facility (*4*) developed by the Army Research Laboratory is an indoor experimental facility located at Aberdeen Proving Ground, MD. The facility, originally designed as a gun test range, has been adapted for reactive materials research. Figure 1 illustrates the layout of the range. Reactive material test samples are right circular cylinders with a nominal diameter and length of 0.503 in. Samples tested are comprised of an aluminum-nickel matrix, with some samples having a tertiary element such as copper or magnesium to vary material properties. The range gun consists of a 30 mm smooth bore powder gun which launches the reactive material sample via a two-piece plastic sabot. Muzzle velocity is nominally 1615 m/s. This is achieved through the use of 109 g of M30 propellant. Approximately 8 ft from muzzle exit a stripper plate is incorporated to terminate the flight of the sabot. Along the flight path velocity measurement devices, break or light screens, are positioned to measure projectile velocity. Break screens were the velocity measuring device of choice and placed 10–12 ft from muzzle with a separation of 3.28 ft. Initially, light screens were used, however, they tended to have a problem picking up muzzle flash and strobe lighting from a safety signal, and therefore where abandoned early in the testing process. Approximately 23 ft from the muzzle is the entrance to the closed testing chamber where the energy release event

occurs. At one point in testing, the distance was increased in order to place the gun and subsequent muzzle blast in a separate room. However, due to the projectile design, dispersion issues became apparent and the RM samples were not always striking the impact plate. Therefore, the gun was moved back to its original position.

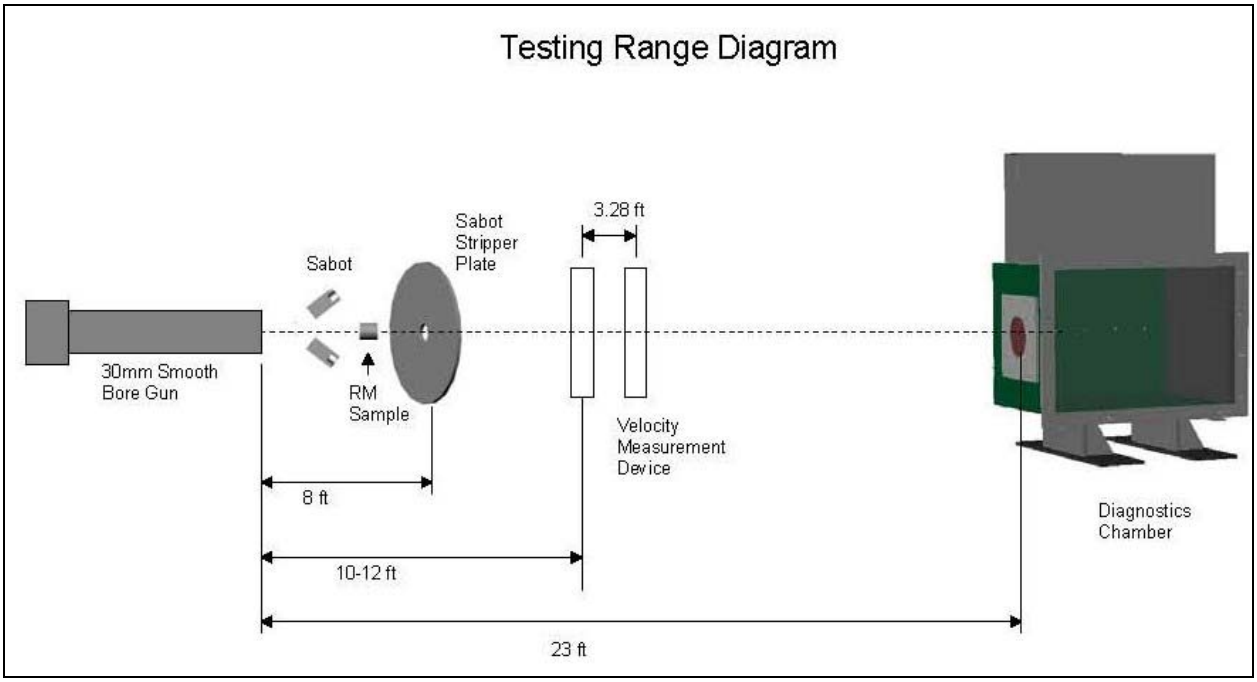

Figure 1. Test facility diagram.

The testing chamber (figure 2) is the focus of the diagnostic suite used to characterize the reactive material combustion event. This chamber is a derivation of the Navy's reactive material test chamber (*1*), but with optical enhancements. The chamber is a 5-sided rectangular steel enclosure measuring 33"Lx21"Hx21"W. Appendix A contains the engineering drawings associated with the chamber. The projectile enters the chamber through a six inch diameter opening, which prior to testing is covered by a witness plate. The plate thickness can vary from 1/32" up to ½" of material, generally steel or aluminum. At the back of the chamber is a 1" thick RHA anvil. In order to contain and view the event, the open (optical front) side of the chamber is sealed with a gasket, sacrificial ¼" thick acrylic sheet, and then 2" polycarbonate cover and fastened with bolts. The top, bottom, and optical rear of the chamber are equipped with five oversized ports each which can accommodate instrumentation to monitor the event inside the chamber. Unused ports are sealed with threaded steel plugs. At the optical rear of the chamber is a customized assembly containing x-ray film cartridges and retro-reflective paper to aid in data acquisition. From the chamber's optical rear to front, this assembly consisted of x-ray cartridges, a protective quarter inch thick acrylic, reflective paper, and finally another sacrificial piece of quarter inch acrylic to protect the assembly from the combustion event. Figure 3 illustrates this configuration. This modular assembly allows for quick access to the x-ray film for processing

and only requires the replacement of the outermost acrylic sheet which is exposed to the combustion event.

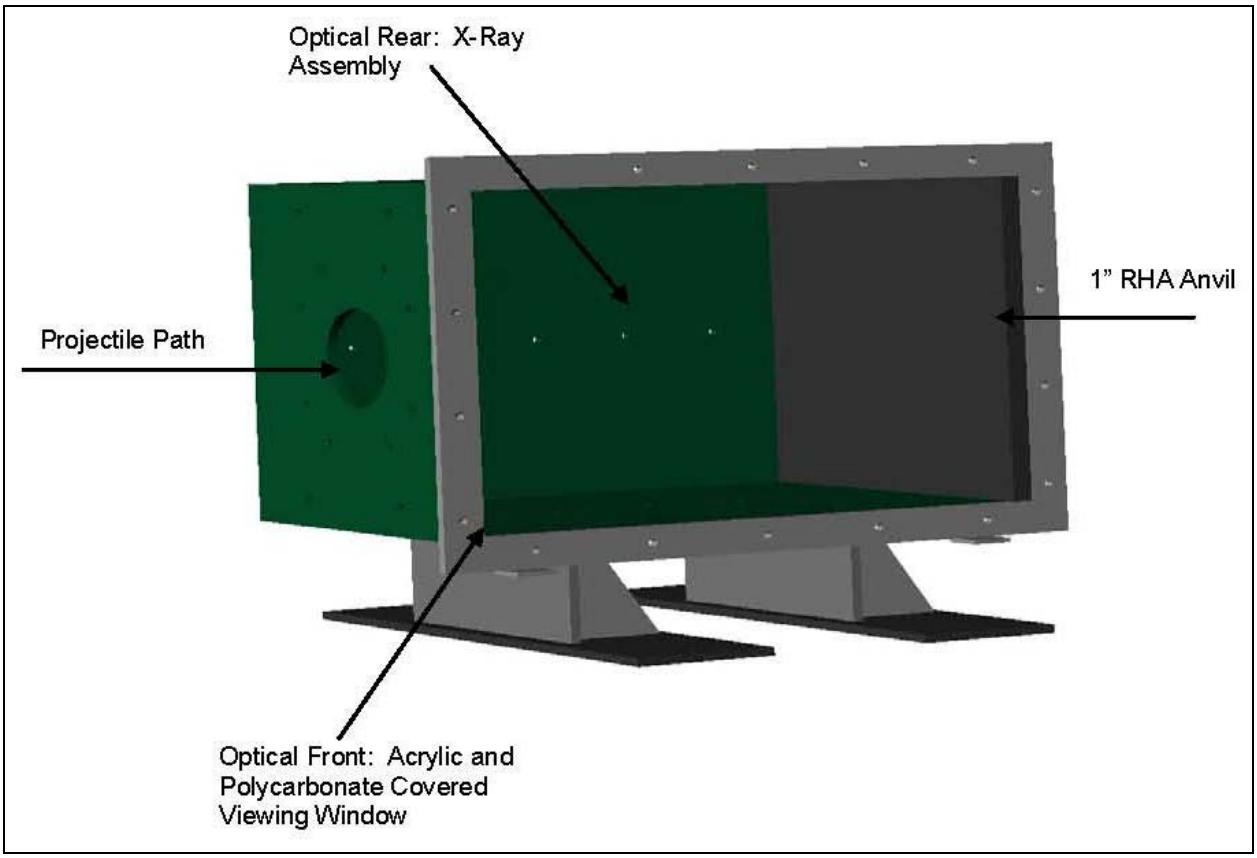

Figure 2. Diagnostics test chamber.

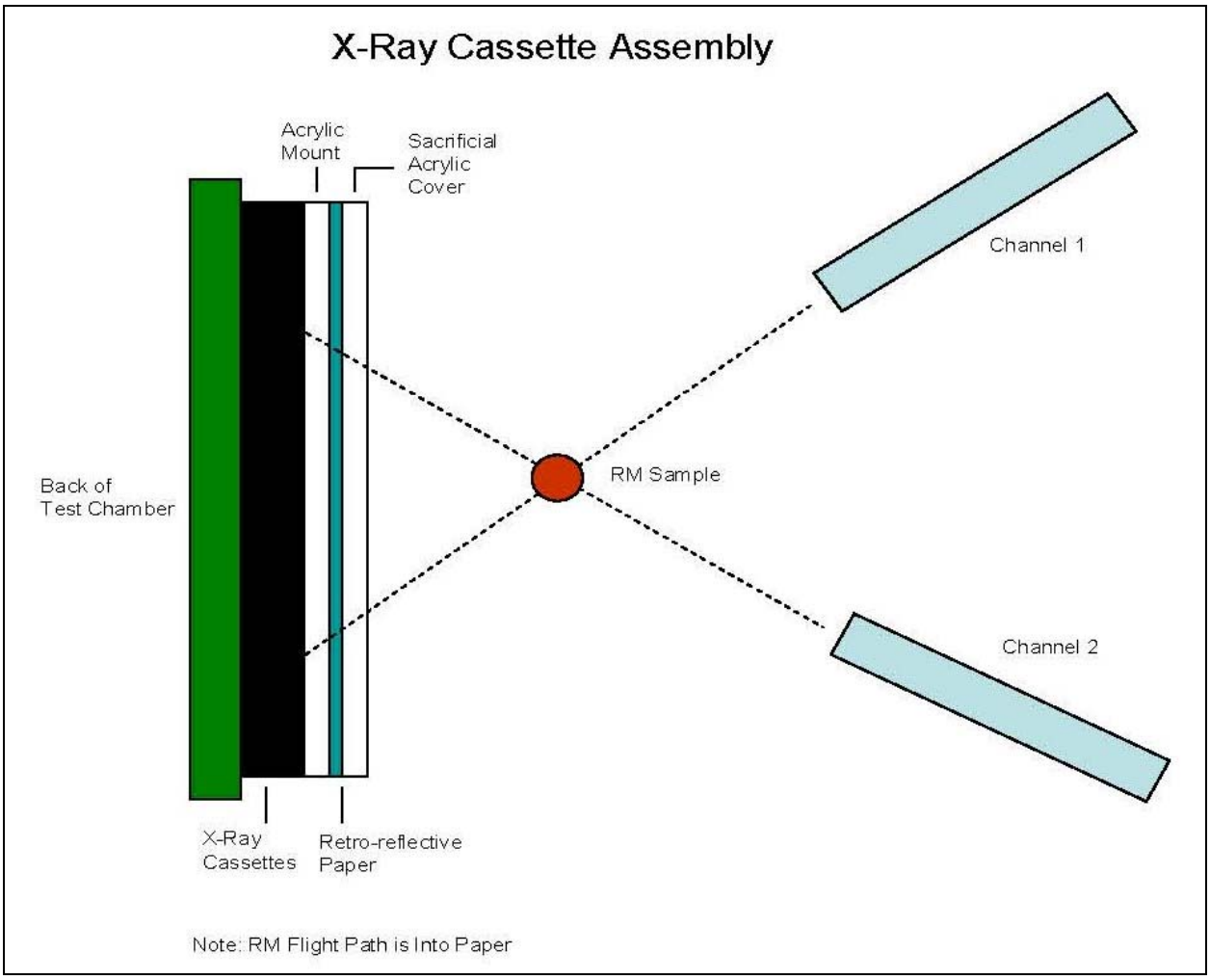

Figure 3. X-ray cassette assembly.

After the reactive material sample is launched from the gun, it first penetrates the witness plate, where the sample is pulverized into a debris field of particles. The material particles continue to travel to the back of the testing chamber where they ultimately impact the anvil and release the majority of their energy. While evidence shows material does react upon impact of the witness plate, the primary combustion event occurs at the anvil. Furthermore, as the debris cloud of particles travels towards the anvil, aerodynamic drag separates the particles according to size with the larger ones impacting the anvil first as the particles are the same density and are near spherical in shape.

The diagnostics time zero trigger is controlled by a break screen placed on the front of the witness plate. This assures consistent triggers when the projectile first impacts the testing chamber. The signal is relayed through a conditioning box which triggers the various cameras, oscilloscopes, and x-ray equipment incorporated to record the test data.

The main diagnostic tools incorporated to characterize the event consist of high speed imaging, emission spectroscopy, pyrometry, pressure measurements and radiography. Due to limited space, a series of lenses and/or mirrors are integrated to direct the desired event images to the cameras. To aid in imaging, an Oxford copper vapor laser is incorporated as are PF-300 Megga-Flash flash bulbs for lighting purposes. Due to the hazardous nature of such a test, the majority of diagnostics are situated outside of the testing range in control rooms, and the event is viewed through an optical port which separates the main control room from the range. Figure 4 shows the optical diagnostic tools used in characterizing the combustion event in the main control room.

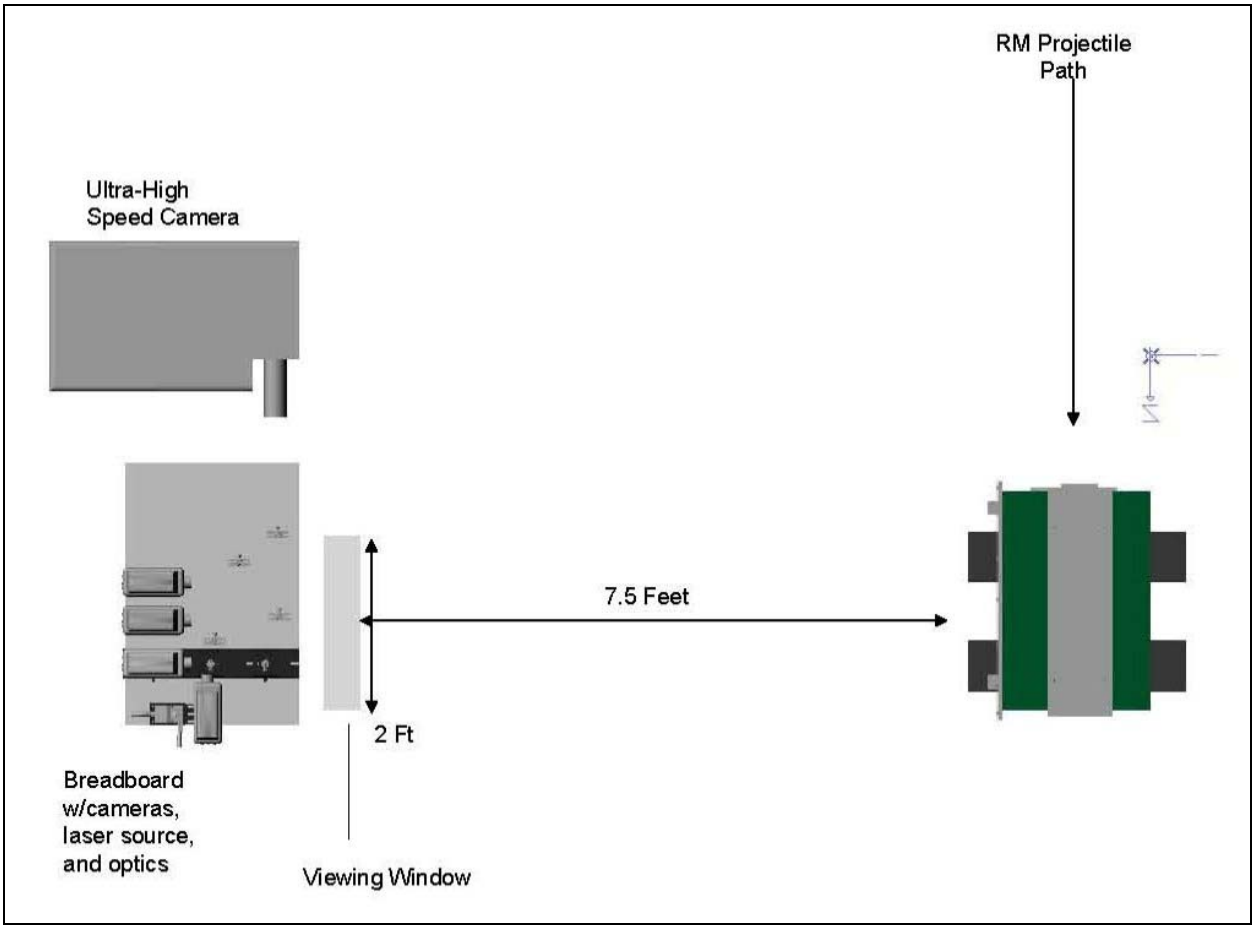

Figure 4. Schematic of optical equipment in control room with relation to diagnostic chamber.

3. Data Measurements

3.1 Pressure

An Agilent MSO8000 series oscilloscope is used to record pressure measurements from PCB Piezotronics Model 101A06 gauges. Measurements are taken by using four of the five port holes

on the top side of the test chamber. The port plugs being used were machined to accept the pressure gages (figure 5). To reduce errant thermal effects caused by combustion, the gauges are coated with grease. A custom fairing was fabricated and installed to protect the gauges and wires from the muzzle blast. Initial testing showed an unacceptable level of noise caused by vibrations from the slug's impact. To mitigate this problem, we fabricated an isolation sleeve out of Delrin® to separate the pressure gage and the steel plug which held the gage. Subsequent testing showed the Delrin® sleeve successfully eliminated the noise.

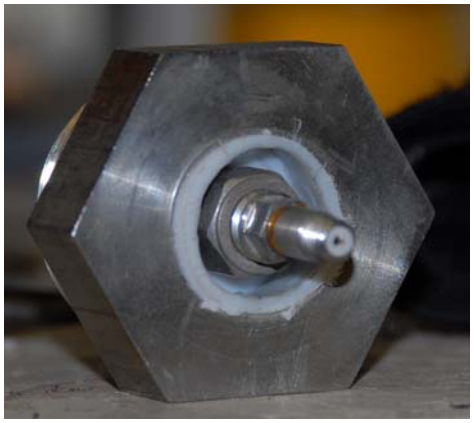

Figure 5. PCB gage mounted in plug with Delrin® isolating sleeve.

3.2 High Speed Imaging

High speed imaging measurements provide a spatial representation of the reactive material's combustion event, and are an integral part of the characterization process. Three distinct high speed imaging techniques are incorporated into the testing process; regular high speed, ultra high speed, and high brightness imaging.

Regular high speed imaging is accomplished using Vision Research's Phantom series camera. The frame rate is set as high as possible once the desired field of view and resolution are set. As the frame rate is increased, the resolution the camera provides will decrease due to the information processing rate of the imaging chip. So while the cameras are capable of imaging well beyond the 17,000 fps, it would not be possible to capture the desired field of view. To provide adequate lighting, two PF-300 flash bulbs are placed near the outside edges of the test chamber and directed towards the event. The flash bulbs provide peak illumination at 30 ms with 6 million lumens of power each. This imaging technique is most practical in showing the entry of the material sample into the test chamber through the impact plate and the flight path of the subsequent debris field towards the anvil. Once the reactive material begins to combust on the anvil, the light intensity of the reaction saturates the camera.

The ultra high speed imaging is accomplished with a Cooke Corporation's HSFC Pro unit. The unit uses a single optical input and a series of beam splitters to transfer light to the four CCD cameras. The cameras are capable of capturing two frames each for a total of eight frames per

testing shot. Each camera is capable of capturing images with an exposure time as fast as 3 ns with zero delay between cameras. This equates to the possibility of capturing images at approximately 300 million frames per second, albeit only with a four frame sequence. The minimum time delay between two images captured on a single channel is 500 ns. In testing the reactive materials, a more modest exposure time of 1–2 μs was used with a 15 μs delay between images. This provided eight images of the combustion event over a 105 μs time span, which is effectively 70k fps, about four times faster than the 'regular' high speed imaging. Figure 6 depicts an image from the ultra high speed camera which represents data collected from channel 4 of the system. In this sequence each camera was used to capture two images each. The top image corresponds to image number four while the bottom represents image number eight in the sequence of eight images captured for the test shot.

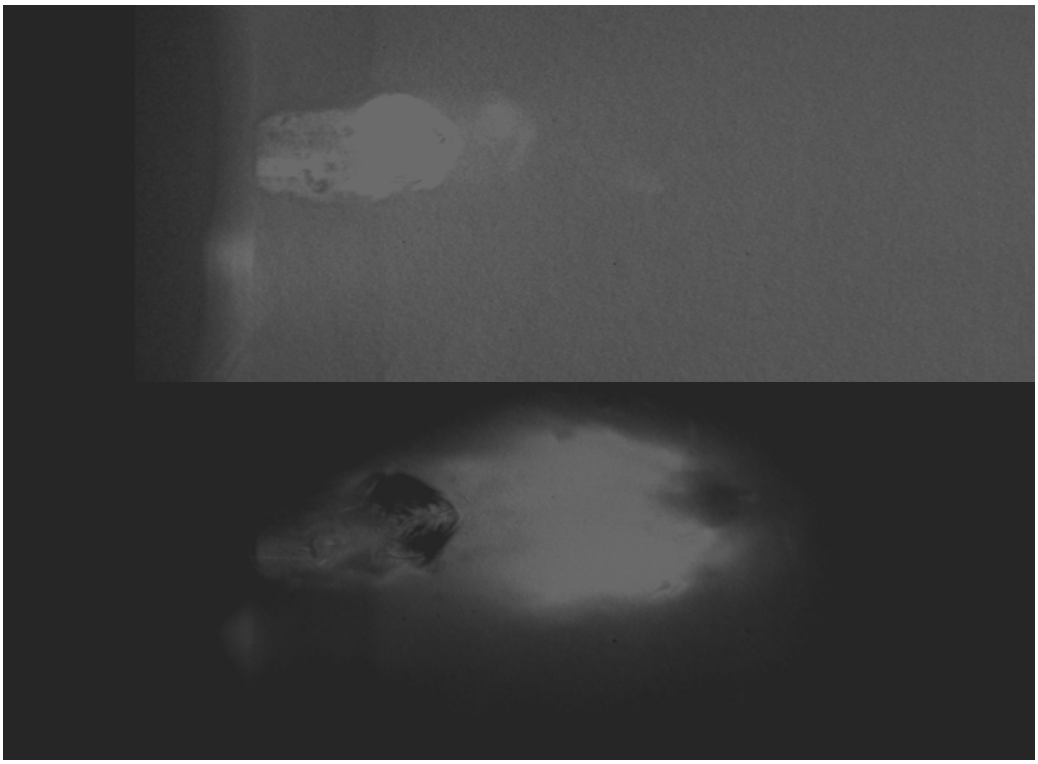

Figure 6. Ultra high speed imaging; time 45 μs (top) and 105 μs (bottom) from t_0.

The third high speed imaging technique incorporated into the diagnostics suite is high brightness imaging (*5*). In this technique, light from a copper vapor laser, emitted at 511 and 578 nm, is directed into the test chamber through a fiber optic cable and series of lenses. The laser light is reflected off of the optical rear of the test chamber, which is fitted with a retro-reflector. The reflected laser light is then imaged by a phantom camera that is filtered at 510 nm. The laser nominally operates at 12.5 kHz with 20 ns pulse duration, but through external syncing can continuously run up to 20 kHz. Nominal energy output is 20 Watts; however, output is adversely affected by the fiber optic used to transport the light as well as running the laser at higher frequencies. Additionally, the laser features a burst mode which can provide light up to 50 kHz

for a one second maximum burst. Images are captured by syncing a high speed Phantom camera to the laser. A delay generator is used to synchronize the camera shutter to the output of the laser. It has been found that a delay of 6–8 μs is needed to sync the exposure to the laser. The camera is also fitted with a band pass filter at 510 nm ± 5 nm, effectively filtering out all but the laser light. Because this technique removes the majority of interfering light from the fireball, particles and shock waves, normally hard to see in standard imaging, can be discerned. In essence, this technique produces a high speed shadow graph of the event with one frame from a typical movie shown in figure 7. High brightness imaging is nominally captured between 15,000 and 20,000 fps, although using the burst mode can produce images up to 50,000 fps.

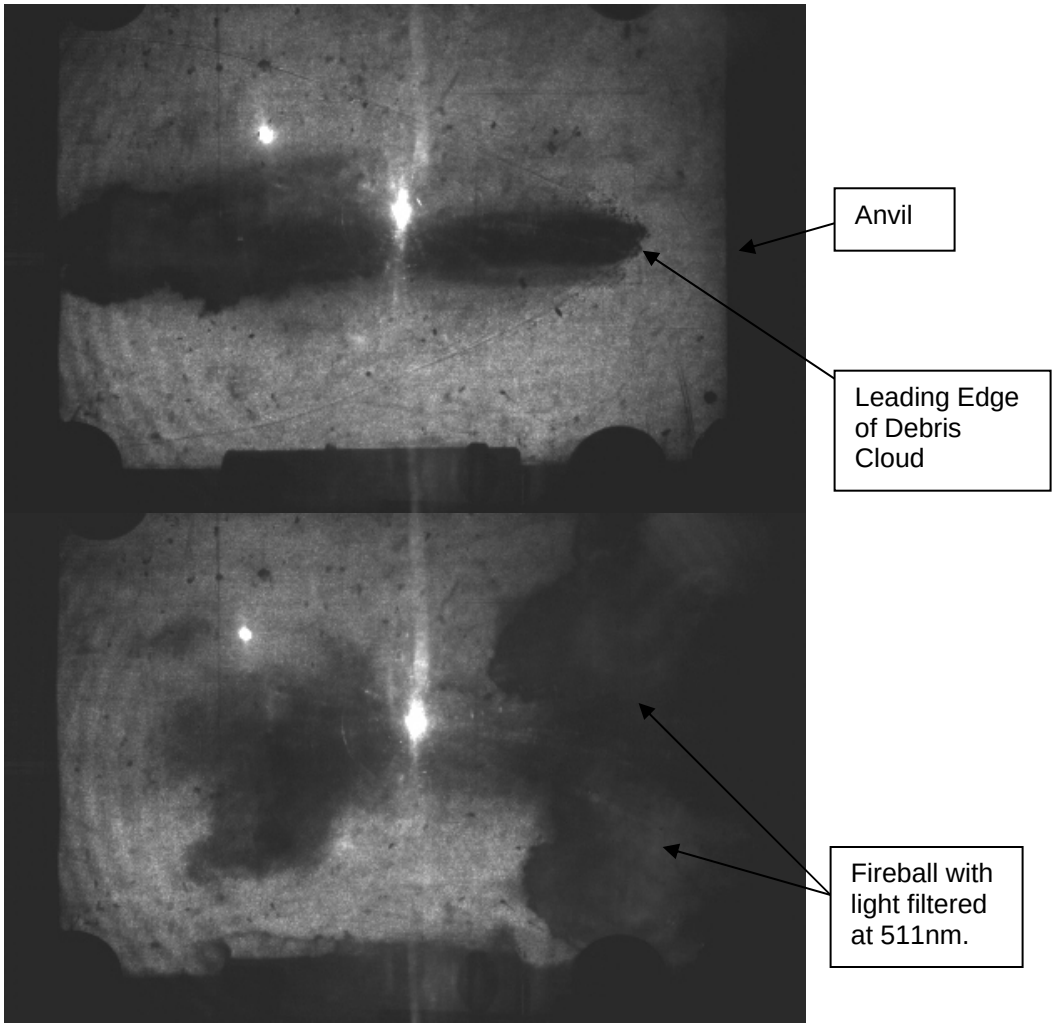

Figure 7. High brightness images. Top: before anvil impact, bottom: after anvil impact.

3.3 Pyrometry

A temporal temperature profile of the reaction event is generated by using two high speed cameras. The cameras are coupled with a beam splitter in order to produce identical imaging

through one optical input. One camera is mounted rigidly on an optical breadboard. Because the intensity from corresponding pixels in each camera are ratioed to determine temperature, image registration is critical. To this end, the other camera is mounted using a Newport-460P-XYZ mounting base, which allows for three degrees of translational motion. The cameras are equipped with band pass filters at 700 nm and 900 nm, respectively (figure 8). The bandwidth of the filters is 10 nm. Data collection for this setup is typically between 1000 and 5000 fps.

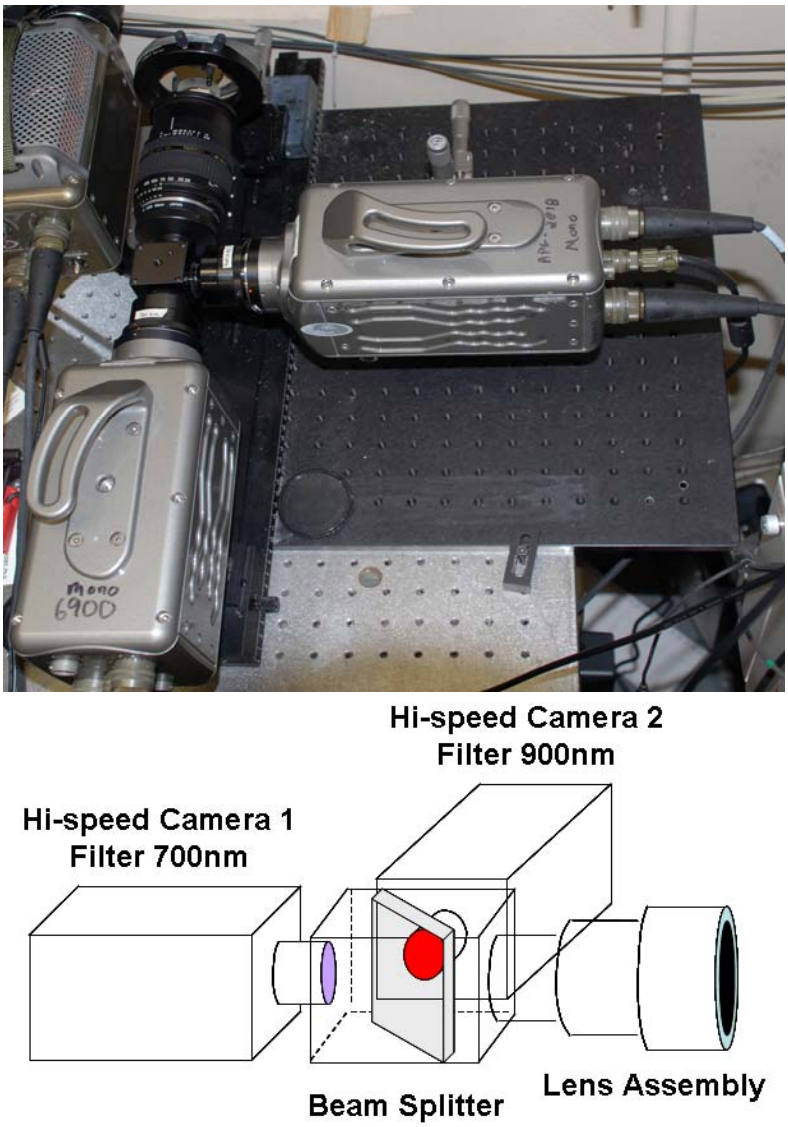

Figure 8. Phantom cameras incorporated for pyrometry.

Temperature profiles were generated from the data through the use of Planck's Law (*6*),

$$I(\lambda,T)=\frac{2hc^2}{\lambda^5}\frac{1}{e^{\frac{hc}{\lambda kT}}-1};$$

where I is spectral radiance, h is Planck's constant, c is the speed of light, λ is wavelength, T is temperature, and k is Boltzmann's constant. A temperature profile can be produced by applying Planck's law to the ratio of intensities recorded on the cameras for an event. Using MATLAB software, we developed a custom in-house code to import the two image files per shot, perform pixel registration to align the images, and execute the necessary calculations in order to produce temperature profiles and histograms of the reaction event (figure 9). The grey body assumption, used to apply Planck's law to real systems, was used in the calculations. We calibrated the system prior to testing using an Omega BB-4A blackbody source with an operating temperature up to 1800 ^{o}F. This image provides both a temperature and pixel registration reference for the two cameras which is then used in the data reduction program.

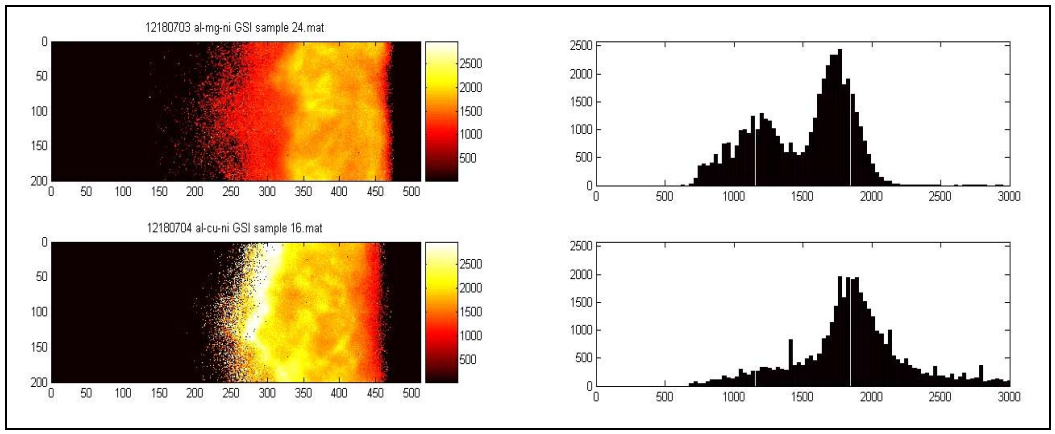

Figure 9. Top: Al-Ni-Mg sample composition, bottom: Al-Ni-Cu sample composition. Left: temperature profile of processed pyrometry data at t=1.4 ms. Color scale represents temperature in Kelvin. Axes are units of arbitrary distance. Right: corresponding histogram in Kelvin.

3.4 Emission Spectroscopy

In an attempt to quantify the gas phase chemistry involved in the process, we incorporated high speed emission spectroscopy into the suite of diagnostics. This experimental rig is designed to spectrally resolve light emitted from different regions of the enclosed chamber during energy release. Specifically, this rig is engineered to measure certain gas phase products of metals (AlO, MgO, ZnO, NiO, etc.) burning in air. Since these metal combustion species occurs in the gas phase only at high temperatures, their measured discrete emission is always accompanied by a thermal greybody continuous emission from nearby hot solid particles.

The experimental setup uses four fiber optic cables (600 micron core Si-Si) that "stare" at different regions of the experimental chamber, looking through the polycarbonate chamber window (*6*). The light emitted during energy release is collected onto the individual fibers (22 degree acceptance angle) and delivered to an imaging spectrograph, a Princeton Instruments Acton Series 320Pi. Light from each fiber is focused onto a different physical portion of a diffraction grating and dispersed onto different regions of the chip of a high speed Phantom

camera. Typical framing rates are 15,000 fps. Calibration is by Cu vapor laser radiation described earlier. Figure 10 shows the components of this setup.

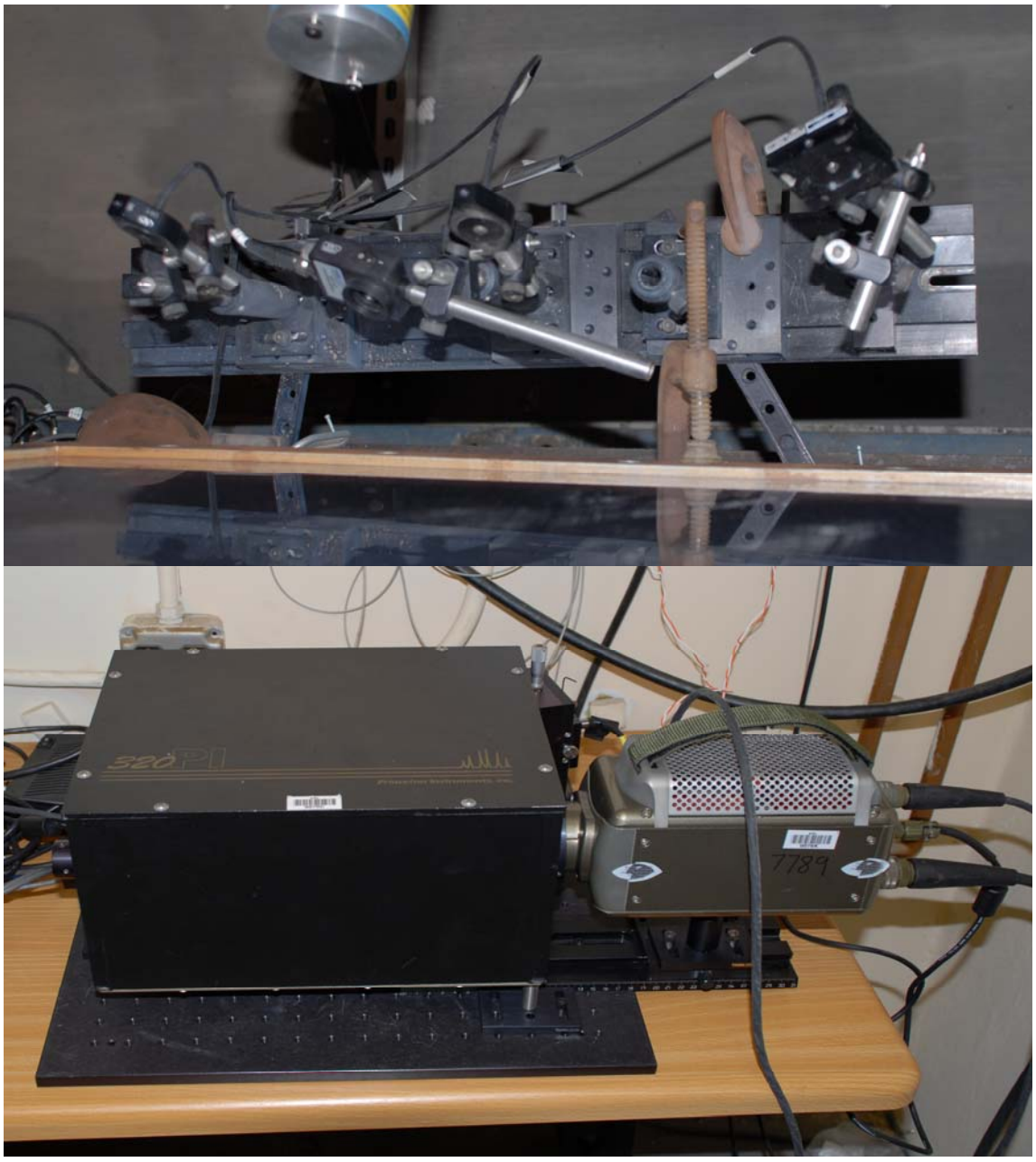

Figure 10. Emission Spectroscopy Instrumentation. Top: overhead view of the photon collecting diodes 'staring' into chamber, Bottom: Spectrometer with Phantom camera.

Data from this event is processed using MATLAB and a custom in-house code in a similar manner as the pyrometry data reduction. The recorded images from the event are imported into MATLAB, with individual frames being converted to spectra. The data can then be processed to generate numerous plots of interest which depict the relationship between wavelength, intensity, and time. From this data a single wavelength of interest can be extracted to determine species'

specific information. Similar plots are produced for all regions of interest; impact plate, chamber center, and anvil

3.5 Radiography

We took digital flash x-rays of the projectile as it initially enters the chamber using a 150 kV L3 Communications pulsead x-ray unit. In total, four channels were incorporated to image the debris cloud at four discrete times as it progressed toward the anvil. The x-ray imaging heads were situated 8–12 in from the polycarbonate window of the test chamber (figure 11). Typically images have been obtained by using a 30kV pulse. To use the limited space available, two images were projected onto one x-ray film. Also, in order to maintain an optical line of sight for the cameras, the x-ray heads were positioned in a manner above and below the shot line, then angled in order to capture the event. This angular mounting creates a vertical separation of the two images on the single film. Since the heads were on the same vertical plane but timed discretely, there was also a horizontal separation of the images. These vertical and horizontal mismatches on one x-ray film make it possible for two distinct images to be read. For example, figure 12 shows a sample x-ray image from the first cassette in the chamber. When processed the images are arranged vertically, but for presentation purposes the images were placed side by side. Located in the cassettes was a lead marker (one ‘L’, one ‘R’) indicating the left and right cassette. This marker made it easy to distinguish orientation of the processed image as well as provide a scale. To protect the cassettes from the reaction event, a sacrificial acrylic window was placed over the assembly. The cassette and protection window where fastened to the back of the testing chamber using standard bolts.

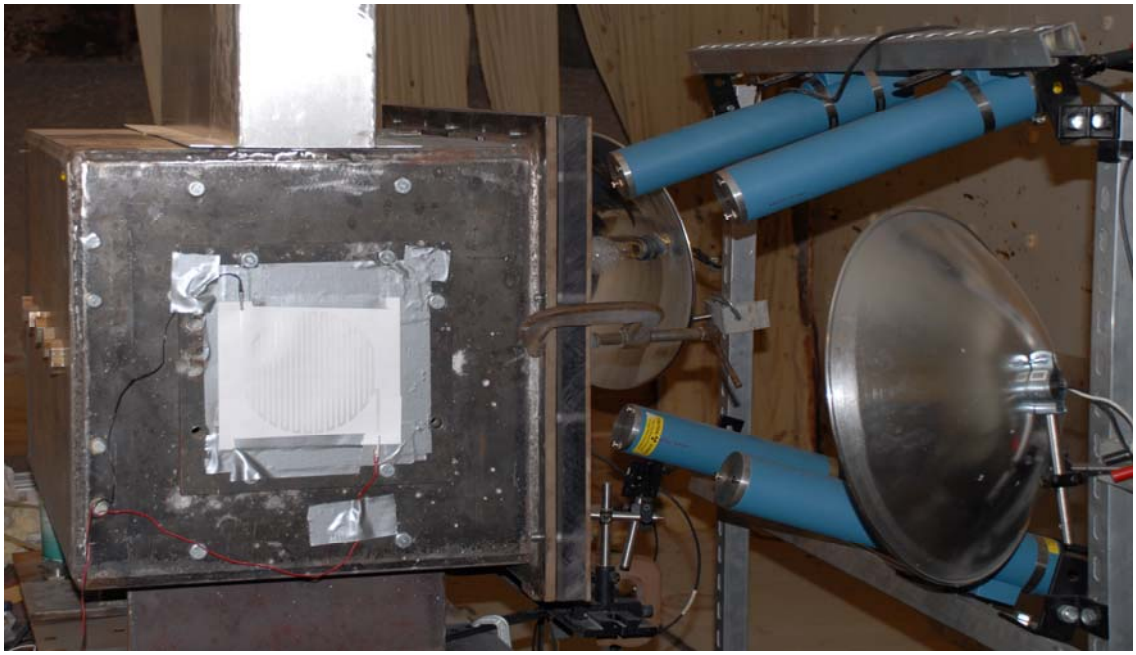

Figure 11. Test Chamber prior to shot. Note x-ray heads angled to maintain optical LOS into chamber, flash bulbs adjacent to heads, and fairing on top to protect pressure gages/wires from shot blast.

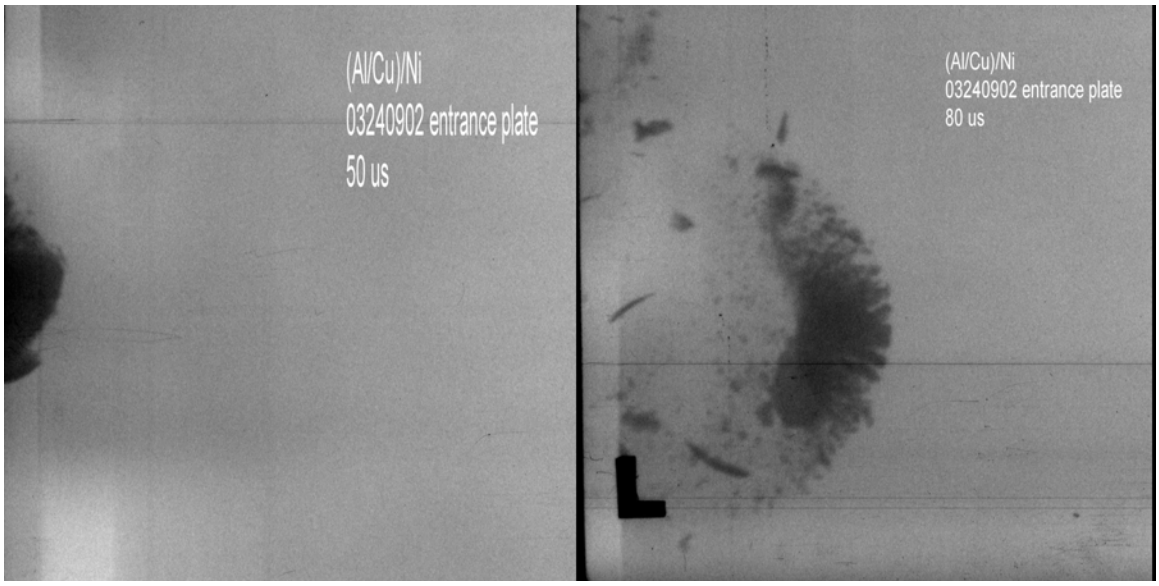

Figure 12. X-Ray image of Al/Cu-Ni sample.

Results have shown promise in producing images that illustrate a detailed image of the reactive material debris field. From these images, it is possible to determine particle sizes within the debris field. Furthermore, because x-rays are attenuated (*7*) as they pass through a material, the opacity of the imaged fragments can be used to estimate the size of the fragments in the direction along the x-ray beam, therefore generating a more accurate three dimensional determination of particle size. As the knowledge base of the system expands, higher fidelity images will be produced to give greater insight into the debris field characteristics.

4. Conclusions

By using an array of diagnostic tools such as pressure measurements, pyrometry, emission spectroscopy, high speed imaging, and radiography, data can be collected and processed to characterize the energy release of a reactive material. Pyrometry measurements provide a time based temperature profile of the energy released. Emission spectroscopy gives insight into the products of combustion. Finally, the multiple high speed imaging techniques along with flash x-ray provide a detailed spatial and temporal resolution of the reactive material's energy release process. Using the processed data ascertained from these testing methods, materials with desirable characteristics can be chosen and integrated into current weapons systems to enhance lethality or produce other desirable effects while maintaining system insensitivity.

5. References

1. Ames, R. Naval Surface Warfare Center Program Summary, XB-NSWCDD/VA, (2003).
2. Richards, D. W.; Kramer, M. P.; Wilson, W. H. Air Force Research Laboratory Technical Report, AFRL-MN-EG-TR-2004-7013 (2003).
3. Homan, B. E.; McNesby, K. L.; Ritter, J.; Colburn, J.; Brant, A. *Characterization of the Combustion Behavior of Aluminum-Nickel Based Reactive Materials*; ARL-TR-4917; U.S. Army Research Laboratory: Aberdeen Proving Ground, MD, 2009.
4. Homan, B. E.; McNesby, K. L.; Pandey, R.; Ritter, J.; Colburn, J.; Brant, A. *Fundamental Mechanism of Energy Release in Reactive Materials*; ARL-TR-4524; U.S. Army Research Laboratory: Aberdeen Proving Ground, MD, 2008.
5. McNesby, K. L.; Homan, B. E. *Real-Time Optical Measurements for Improved Understanding of Enhanced Blast Materials*; ARL-TR-3483; U.S. Army Research Laboratory: Aberdeen Proving Ground, MD, 2005.
6. McNesby, K. L.; Homan, B. E.; Piehler, T. N.; Lottero, R. E. *Spectroscopic Measurements of Fireballs Produced by Enhanced Blast Explosives*; ARL-TR-3318; U.S. Army Research Laboratory: Aberdeen Proving Ground, MD, 2004.
7. Hubbell, J. H. Bibliography of Photon Total Cross Section (Attenuation Coefficient) Measurement 10 eV to 13.5 eV. 1907-1993, NISTIR 5437, 1994.

Appendix A. Test Chamber Drawings

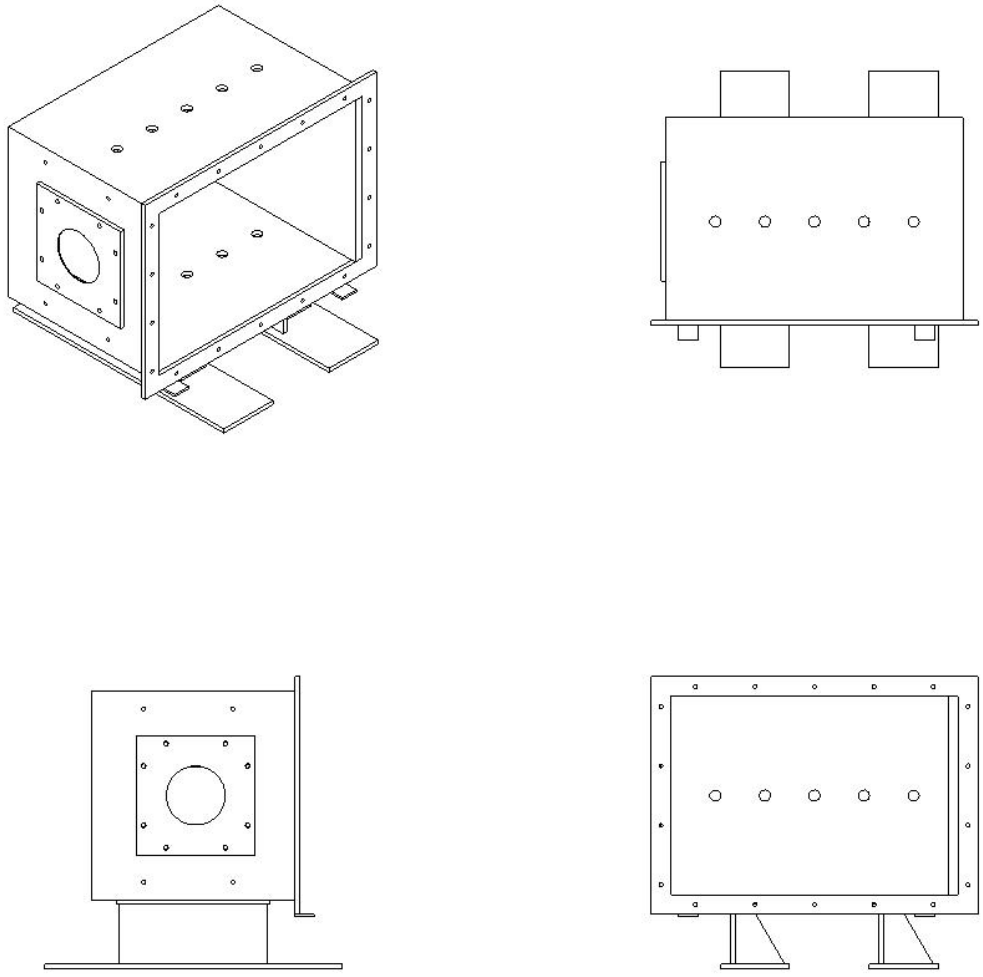

Diagnostic Chamber Assembly

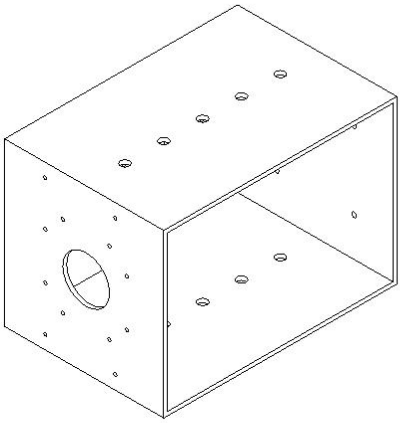

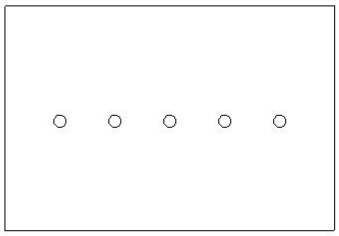

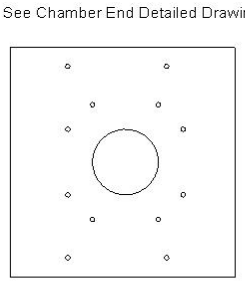

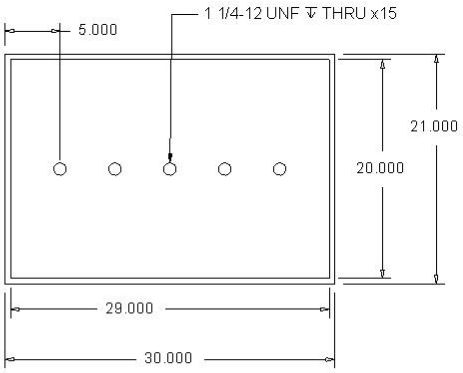

Main Chamber
Material: Steel

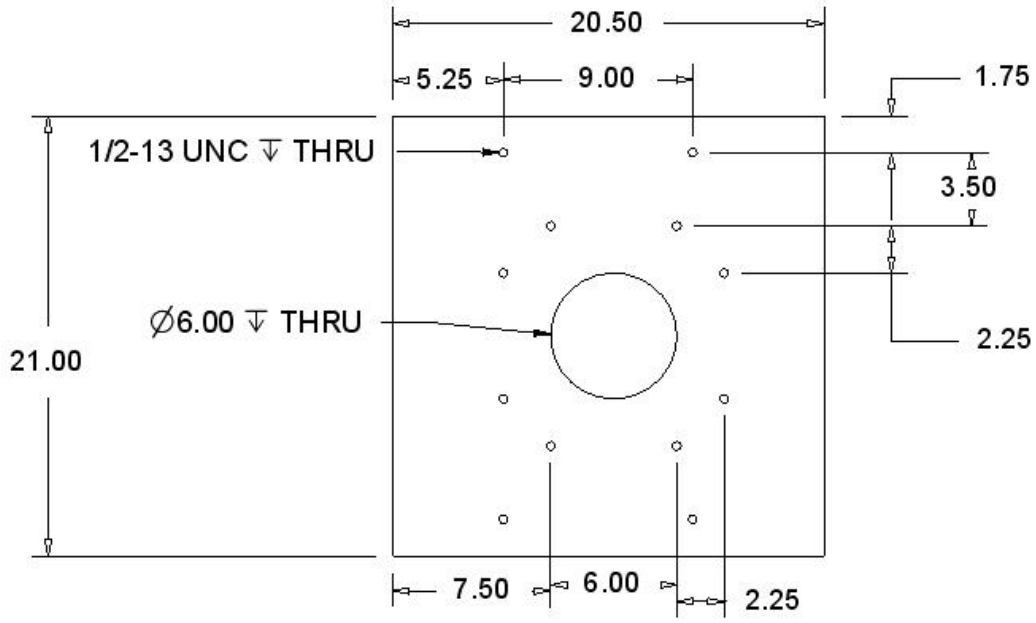

Detailed End of Chamber Drawing

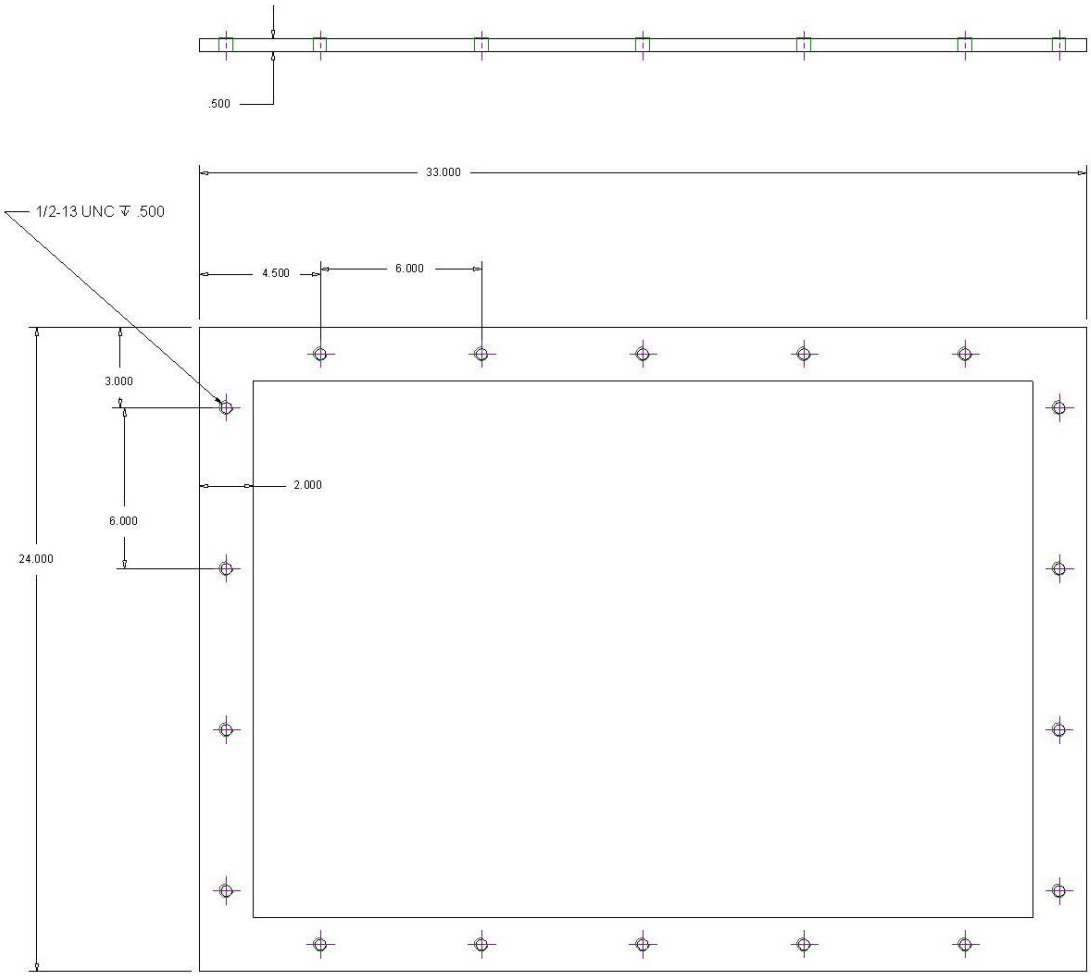

Chamber Flange
Material: Steel

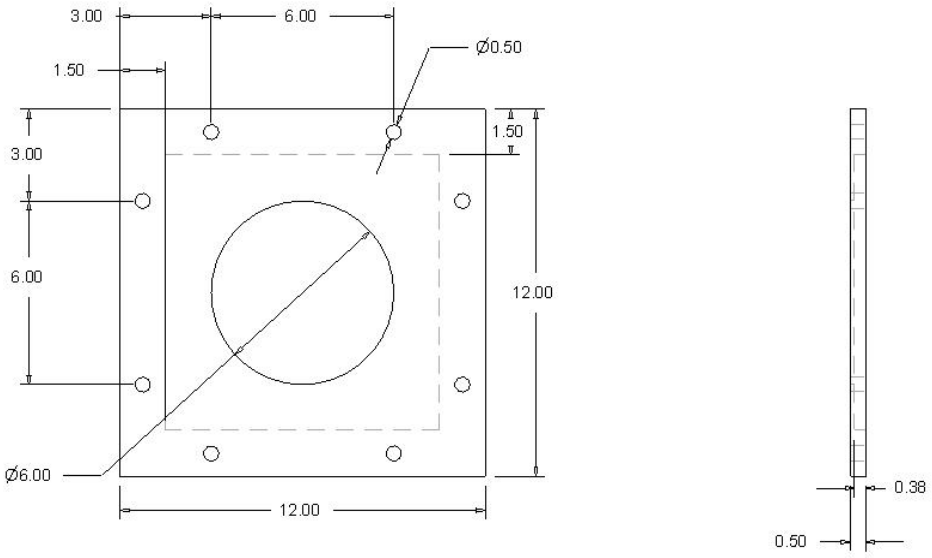

Target Plate Holder
Material: Aluminum

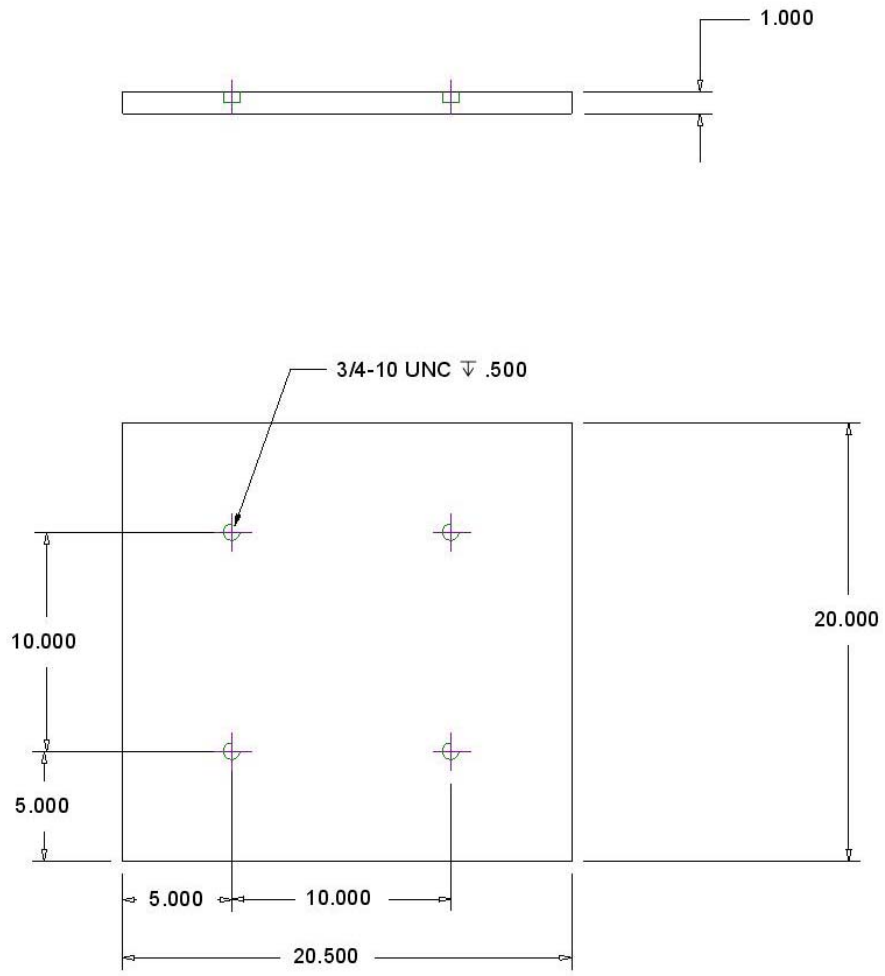

Anvil
Material: RHA

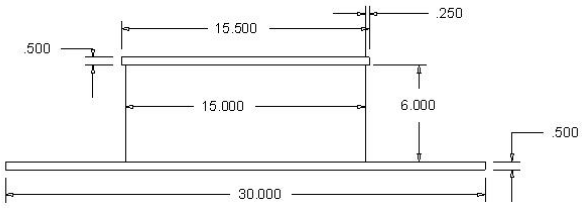

Front

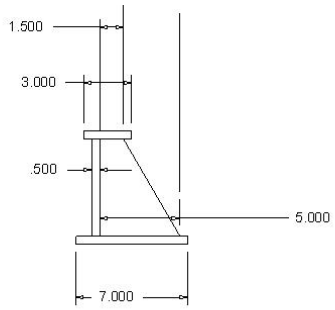

Right

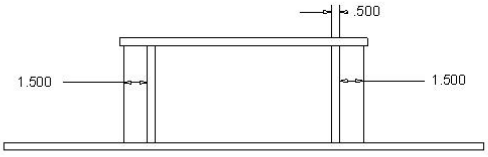

Back

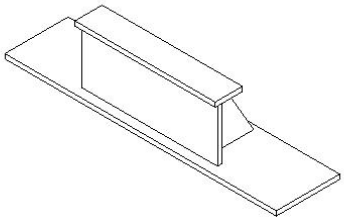

Mount
Material: Steel
All Joints Welded

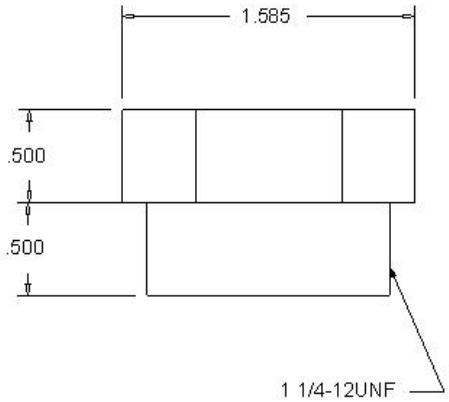

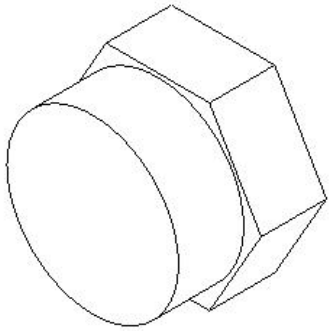

Plug
Material: Steel

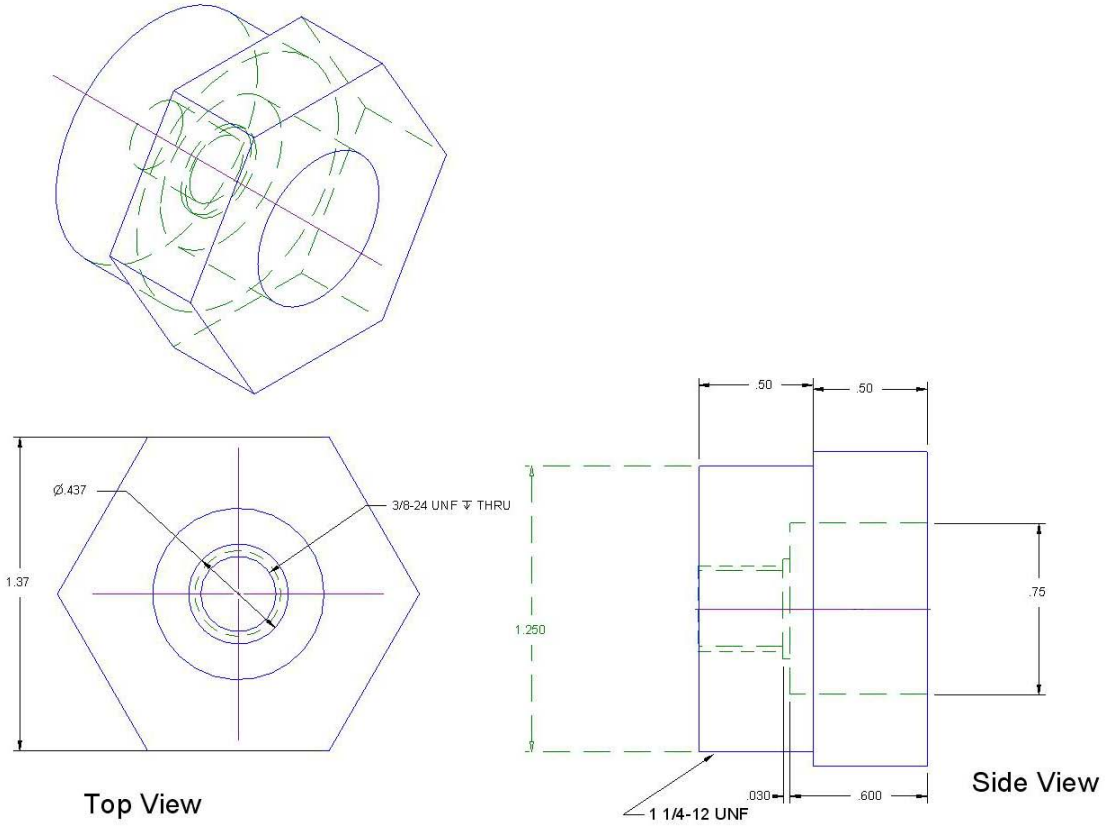

Plug Modified to Accept PCB Pressure Gage

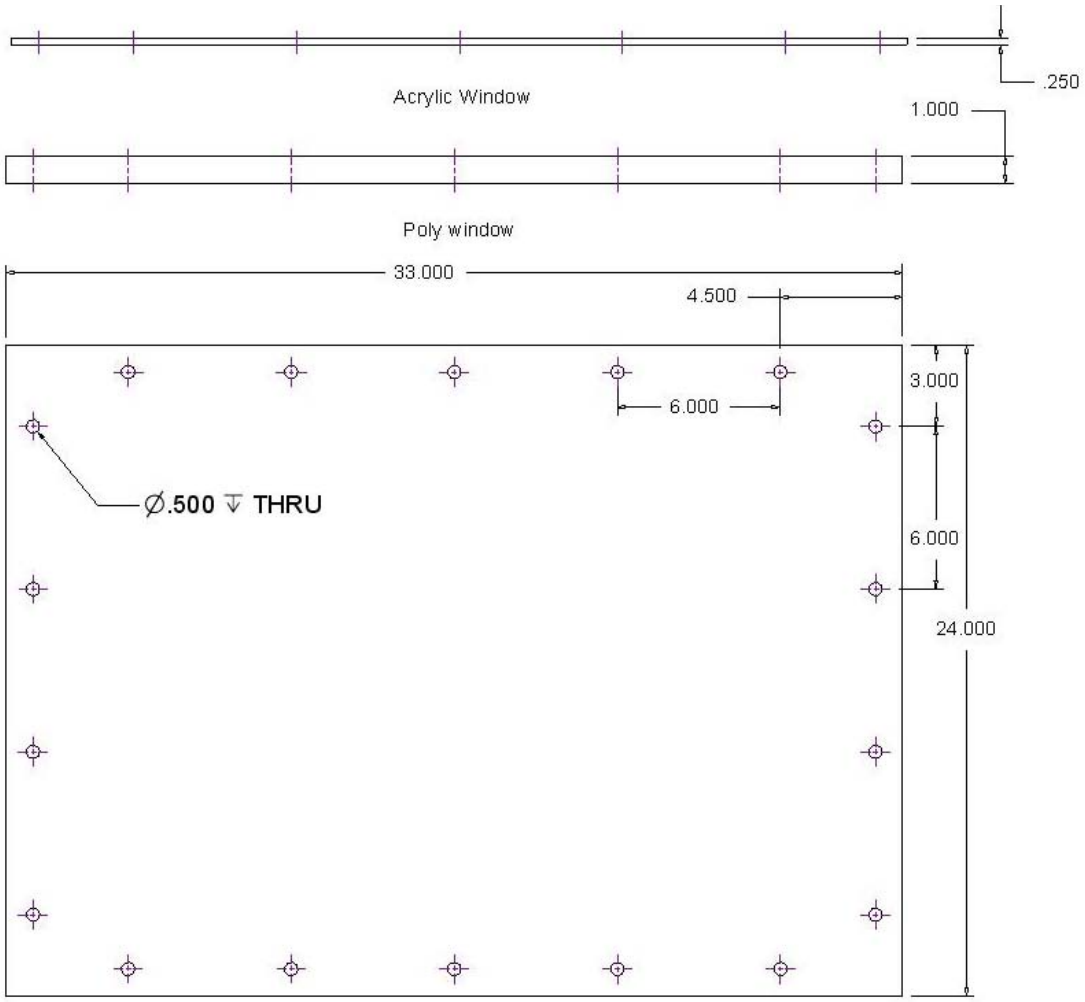

Chamber Windows

1 (PDF ONLY) DEFENSE TECHNICAL INFORMATION CTR
DTIC OCA
8725 JOHN J KINGMAN RD
STE 0944
FORT BELVOIR VA 22060-6218

1 DIRECTOR
US ARMY RESEARCH LAB
IMNE ALC HRR
2800 POWDER MILL RD
ADELPHI MD 20783-1197

1 DIRECTOR
US ARMY RESEARCH LAB
RDRL CIM L TECHL LIB
2800 POWDER MILL RD
ADELPHI MD 20783-1197

1 DIRECTOR
US ARMY RESEARCH LAB
RDRL CIM P TECH PUBS
2800 POWDER MILL RD
ADELPHI MD 20783-1197

1 DIR USARL
RDRL ROP TECH LIB
PO BOX 12211
RESEARCH TRIANGLE PARK NC
27709-2211

1 US ARMY
PEO AMMO PMCAS
SFAE AMO CAS
J IRIZARRY
BLDG 171A
PICATINNY ARSENAL NJ 07806-5000

1 COMMANDER
RADFORD ARMY AMMO PLANT
SMCAR QA HI LIB
RADFORD VA 244141-0298

1 DIR BENET WEAPONS LAB
TECH LIB
WATERVLIET NY 12189-4000

1 CDR NAVAL RSRCH LAB
TECH LIB
WASHINGTON DC 20375-1972

2 OFFICE OF NAVAL RSRCH
C BEDFORD
B ALMQUIST
875 N RANDOLPH ST RM 653
ARLINGTON VA 22203-1927

1 GENERAL SCIENCE INCOPORATED
A ROZANSKI
205 SCHOOLHOUSE ROAD
SOUDERTON PA 18964

ABERDEEN PROVING GROUND

1 DIR USARL
RDRL CIM G (BLDG 4600)

15 DIR USARL
RDRL WML
M ZOLTOWSKI
RDRL WML B
B E HOMAN
R C SAUSA
RDRL WML C
K L MCNESBY
RDRL WML D
R A BEYER
A L BRANT
J COLBURN
RDRL WML H
C CANDLAND
M FERMEN-COKER
R SUMMERS
RDRL WMM D
V CHAMPAGNE
M TREXLER
RDRL WMP B
B MCANDREW
R EHLERS
RDRL WMS
J RITTER

TOTAL: 28 (1 ELEC, 27 HCs)

INTENTIONALLY LEFT BLANK.